Advanced Mathematical Models & Applications
Vol.10, No.3, 2025, pp.488-498
https://doi.org/10.62476/amma.103488

CHAOS SYNCHRONIZATION IN A FRACTIONAL-ORDER COMPUTER VIRUS SYSTEM WITH INCOMMENSURATE DYNAMICS

Shaher Momani[1,2], **Imane Zouak**[3], **Iqbal Batiha**[2,4*],
Adel Ouannas[5], **Amina-Aicha Khennaoui**[6], **Zainah Momani**[7]

[1]Department of Mathematics, Faculty of Science, University of Jordan, Amman 11942, Jordan
[2]Nonlinear Dynamics Research Center (NDRC), Ajman University, Ajman 346, United Arab Emirates
[3]Department of Mathematics and Informatics, University of Larbi Ben M'hidi, Oum El Bouaghi, Algeria
[4]Department of Mathematics, Al-Zaytoonah University of Jordan, Amman 11733, Jordan
[5]Department of Mathematics and Computer Science, University of Larbi Ben M'hidi, Oum El Bouaghi, Algeria
[6]NTIC Faculty, University of Constantine 2, Algeria
[7]Department of Computer Science, University of Jordan, Amman 11942, Jordan

Abstract. This paper investigates the chaotic dynamics and synchronization of an incommensurate fractional discrete computer virus model. Leveraging fractional calculus captures memory and non-local propagation effects observed in real networks. We characterize the system's complex behavior using bifurcation diagrams, phase portraits, and the maximum Lyapunov exponent (MLE), confirming chaos via regimes with $MLE > 0$. We then implement a master–slave coupling to achieve synchronization in the chaotic regime and quantify convergence of the synchronization error. Numerical simulations show that the master system and the slave system synchronize for control parameters $f_1 = -0.34, f_2 = -0.52$ and $f_3 = -0.76$. These results highlight how incommensurate fractional orders shape chaotic windows and demonstrate that appropriately tuned feedback can enforce coherent behavior, offering insights for designing mitigation strategies against computer-virus spread on complex networks.

Keywords: Computer virus model, synchronization, incommensurate fractional-order derivative, numerical simulations.

AMS Subject Classification: 34A08, 34D06, 37N25.

Corresponding author: Iqbal Batiha, Department of Mathematics, Al-Zaytoonah University of Jordan, Amman 11733, Jordan, e-mail: *i.batiha@zuj.edu.jo*

Received: 30 July 2025; Revised: 20 August 2025; Accepted: 2 September 2025; Published: 3 December 2025.

1 Introduction

In the digital age, cyber threats have evolved into a significant global concern. Computer viruses, as one of the primary cyber threats, pose a serious risk to information security Yang & Yang (2012). These malicious software programs can replicate themselves, spread rapidly, and cause severe damage to computer systems (Yang et al., 2013; Ren et al., 2012).

Fractional calculus is one of the sophisticated mathematical tools that researchers have used to address the increasing complexity of contemporary systems (Ouannas et al., 2023, 2022; Talbi et al., 2020a,b). A more thorough description of systems with memory and hereditary properties is made possible by fractional calculus, which extends the ideas of classical calculus, which deals with integer-order derivatives and integrals to non-integer orders (Khennaoui et al., 2019; Ouannas et al., 2019a, 2020, 2019b; Ouannas & Pham, 2019). For modeling real-world phenomena with complex behaviors and long-term dependencies, this robust framework has proven especially helpful (Khennaoui et al., 2019, 2018; Ouannas et al., 2018; Bendoukha et al., 2018; Ouannas & Odibat, 2015a). Scientists and engineers can better capture the dynamics of systems that are difficult to describe with conventional methods by utilizing fractional derivatives and integrals (Ouannas, Azar & Vaidyanathan, 2017; Ouannas & Odibat, 2015b; Anakira et al., 2023; Farraj et al., 2023; Berir, 2024; Dharmalingam et al., 2024; Batiha et al., 2025a,b; Momani et al., 2025).

Incommensurate fractional systems, in which various system components are distinguished by different fractional orders, are among the most fascinating research topics in this field (Ouannas & Al-Sawalha, 2016; Cuomo & Oppenheim, 1993; Ouannas et al., 2019c; Wu & Baleanu, 2014). These systems present special difficulties for analysis and control because they are intrinsically complex and frequently display rich and intricate dynamics (Liu, 2016). Notwithstanding these difficulties, incommensurate fractional systems present a great deal of promise for improving our comprehension of multiscale and nonlinear phenomena (Wu et al., 2016). Additionally, the concept of synchronization has garnered significant interest as a means to address issues with system coordination and secure communication. The process of aligning several systems' behaviors so they can work together harmoniously is known as synchronization (Zhang et al., 2007; Terry & VanWiggeren, 2001; Ouannas et al., 2019d).

In today's interconnected digital world, cyber threats have become increasingly sophisticated and pervasive. Computer viruses, as one of the most prevalent forms of cyberattacks, pose a significant risk to individuals, organizations, and critical infrastructure. As these threats continue to evolve, innovative approaches are needed to safeguard our digital assets. The synchronization of incommensurate fractional discrete computer virus models represents a novel and challenging research direction. By analyzing the synchronization conditions and designing effective synchronization schemes, we can develop robust and secure communication systems that are resilient to cyberattacks.

This research aims to investigate the synchronization of incommensurate fractional discrete computer virus models. By exploring the underlying dynamics and developing innovative synchronization techniques, we seek to contribute to the advancement of cybersecurity and the protection of critical infrastructure.

The paper is organized as follows. Section 2 provides a foundational overview of fractional discrete systems, culminating in the introduction of an incommensurate fractional discrete computer virus model. Section 3 presents the synchronization analysis of the proposed model, including synchronization criteria and numerical simulations to validate the theoretical findings. Finally, Section 4 concludes the paper by summarizing the key contributions and outlining potential avenues for future research.

2 Basic Concepts and Model Description

In this section, we recall some fundamental notions of discrete fractional calculus that will be used throughout the paper. These concepts provide the mathematical framework for describing memory and hereditary effects in dynamical systems. Based on these tools, we then formulate the proposed fractional discrete computer virus model.

2.1 Fractional Discrete Operators

In this subsection, we recall some basic notions of discrete fractional calculus that will be used in the formulation and analysis of the proposed model.

Definition 1. *(Abdeljawad, 2011)The κ-th fractional sum of a function χ can be expressed by*

$$\Delta_b^{-\kappa}\chi(\mathtt{t}) = \frac{1}{\Gamma(\kappa)}\sum_{m=b}^{b-\kappa}(b-1-m)^{(\kappa-1)}\chi(m), \tag{1}$$

where $s \in \mathbb{N}_{b+\kappa}$, $\kappa > 0$, and $\mathbb{N}_b = \{b, b+1, b+2, \dots\}$.

Definition 2. *(Atici & Eloe, 2009) The Caputo-like difference operator for χ is defined by*

$${}^c\Delta_b^{\kappa}\chi(\mathtt{t}) = \Delta_b^{-(l-\kappa)}\Delta^l\chi(\mathtt{t}) = \frac{1}{\Gamma(l-\kappa)}\sum_{m=b}^{\mathtt{t}-(l-\kappa)}(\mathtt{t}-m-1)^{(l-\kappa-1)}\Delta^l\chi(m), \tag{2}$$

such that $\mathtt{t} \in \mathbb{N}_{b+l-\kappa}$, , and $m = \lceil\kappa\rceil + 1$.

The discrete fractional model's numerical formula is introduced by the following theorem.

Theorem 1. *Wu & Baleanu (2014)The solution to the fractional difference system*

$$\begin{cases} {}^c\Delta_b^{\kappa}Y(\mathtt{t}) = \chi(\mathtt{t}+\kappa-1, Y(\mathtt{t}+\kappa-1)), \\ \Delta^i Y(b) = Y_i, \quad l = \lceil\kappa\rceil + 1, \end{cases} \tag{3}$$

is expressed by

$$Y(\mathtt{t}) = Y_0(\mathtt{t}) + \frac{1}{\Gamma(\kappa)}\sum_{m=l-\kappa}^{\mathtt{t}-\kappa}(\mathtt{t}+1-m)^{(\kappa-1)}\chi(m-1+\kappa, Y(m-1+\kappa)), \tag{4}$$

such that

$$Y_0(\mathtt{t}) = \sum_{j=0}^{l-1}\frac{(\mathtt{t}-b)^j}{\Gamma(j+1)}\Delta^j Y(0). \tag{5}$$

The next theorem reveals the key conditions that guarantee the stability of incommensurate fractional-order difference equations.

Theorem 2. *(Shatnawi et al., 2022)*
Consider the following system of difference equations:

$$\begin{cases} {}^c\Delta_0^{\kappa_1}\chi_1(t) = \mathbf{G_1}(\chi(t+\kappa_1-1)), \\ {}^c\Delta_0^{\kappa_2}\chi_2(t) = \mathbf{G_2}(\chi(t+\kappa_2-1)), \\ \vdots \\ {}^c\Delta_0^{\kappa_n}\chi_n(t) = \mathbf{G_n}(\chi(t+\kappa_n-1)), \end{cases} \tag{6}$$

where $\mathbf{G} = (\mathbf{G_1}, \mathbf{G_2}, ..., \mathbf{G_n}) : \mathbb{R}^n \to \mathbb{R}^n$ and $\chi(t) = (\chi_1(t), \chi_2(t), ..., \chi_n(t))^T \in \mathbb{R}^n$. Consider κ_j such that $0 < \kappa_j < 1$ for $\mathrm{j} = 1, 2, \dots, n$. Let M be the least common multiple of the denominators g_j of κ_j, where $\kappa_j = \frac{w_j}{g_j}$ with $(w_j, g_j) = 1$ and $w_j, g_j \in \mathbb{Z}^+$ for $\mathrm{j} = 1, 2, \dots, n$. Define $r = \frac{1}{M}$.

$$\det\left(diag(\lambda^{M\kappa_1}, \lambda^{M\kappa_2}, \dots, \lambda^{M\kappa_n}) - (1-\lambda^M)\mathbf{J}\right) = 0, \tag{7}$$

such that $\mathbf{J}$ is the Jacobian matrix of (6). If at least one root of (7) lie inside the set $\mathcal{C} \setminus K^r$, then the trivial solution of the system (6) is locally asymptotically stable, where

$$K^r = \left\{z \in \mathbb{C} \,:\, |z| \le \left(2\cos\frac{|\arg(z)|}{r}\right)^r, \text{ and} |\arg(z)| \le \frac{r\pi}{2}\right\}, \tag{8}$$

2.2 The Model

Yang et al. (2013) pioneered the study of computer virus dynamics by proposing the following model. In this formulation, the total number of internal computers is normalized so that $S(t) + L(t) + B(t) = 1$, where $S(t)$, $L(t)$, and $B(t)$ denote the percentages of uninfected, latent, and seizing computers, respectively. The model is governed by the system

$$\begin{cases} \dot{S} = \sigma - \beta S(L+B) + \gamma_1 L + \gamma_2 B - \sigma S, \\ \dot{L} = \beta S(L+B) - \gamma_1 L - \alpha L - \sigma L, \\ \dot{B} = \alpha L - \gamma_2 B - \sigma B. \end{cases} \tag{9}$$

All parameters are assumed to be positive. Their biological and technical interpretations are summarized in Table 1.

Table 1: Description of variables and parameters in system (9).

Symbol	Description
$S(t)$	Percentage of uninfected (virus-free) computers
$L(t)$	Percentage of latent (infected but not yet breaking out) computers
$B(t)$	Percentage of seizing (infected and actively breaking out) computers
σ	Connection/disconnection rate of computers
β	Infection transmission rate
α	Rate at which latent computers become seizing
γ_1	Recovery rate of latent computers
γ_2	Recovery rate of seizing computers

The first-order difference of (9) is designed as follows using a discretization:

$$\begin{cases} \Delta S = h[\sigma - \beta S_n(L_n + B_n) + \gamma_1 L_n + \gamma_2 B_n - \sigma S_n], \\ \Delta L = h[\beta S_n(L_n + B_n) - \gamma_1 L_n - \alpha L_n - \sigma L_n], \\ \Delta B = h[\alpha L_n - \gamma_2 B_n - \sigma B_n]. \end{cases} \tag{10}$$

We investigate the behavior of the proposed fractional model with incommensurate order. By assigning different fractional order values, we introduce the concept of incommensurate order and generate a novel incommensurate fractional chaotic model. Using the Caputo-like difference operator ${}^{\mathtt{c}}\Delta_b^{\kappa}$, we create the fractional version of 10.

$$\begin{cases} {}^{\mathtt{c}}\Delta_b^{\kappa_1} S(\mathtt{t}) & = h[\sigma - \beta S(\mathtt{t}+\kappa_1-1)(L(\mathtt{t}+\kappa_1-1) + B(\mathtt{t}+\kappa_1-1)) + \gamma_1 L(\mathtt{t}+\kappa_1-1) \\ & \quad +\gamma_2 B(\mathtt{t}+\kappa_1-1) - \sigma S(\mathtt{t}+\kappa_1-1)], \\ {}^{\mathtt{c}}\Delta_b^{\kappa_2} L(\mathtt{t}) & = h[\beta S(\mathtt{t}+\kappa_2-1)(L(\mathtt{t}+\kappa_2-1) + B(\mathtt{t}+\kappa_2-1)) - \gamma_1 L(\mathtt{t}+\kappa_2-1) \\ & \quad -\alpha L(\mathtt{t}+\kappa_2-1) - \sigma L(\mathtt{t}+\kappa_2-1)], \\ {}^{\mathtt{c}}\Delta_b^{\kappa_3} B(\mathtt{t}) & = h[\alpha L(\mathtt{t}+\kappa_3-1) - \gamma_2 B(\mathtt{t}+\kappa_3-1) - \sigma B(\mathtt{t}+\kappa_3-1)]. \end{cases} \tag{11}$$

where $0 < \kappa_{1,2,3} \leq 1$, $\mathtt{t} \in \mathbb{N}_{b+1-\kappa}$,

Setting $b = 0$ and using Theorem 1, we obtain the numerical formula of the fractional discrete system 11:

$$\begin{cases} S(\mathtt{n}) = S(0) + \frac{h}{\Gamma(\kappa_1)} \sum_{\mathtt{j}=1}^{\mathtt{n}} \frac{\Gamma(\mathtt{n}-\mathtt{j}+\kappa_1)}{\Gamma(\mathtt{n}-\mathtt{j}+1)} & [\sigma - \beta S(\mathtt{j}-1)(L(\mathtt{j}-1) + B(\mathtt{j}-1)) \\ & +\gamma_1 L(\mathtt{j}-1) + \gamma_2 B(\mathtt{j}-1) - \sigma S(\mathtt{j}-1)], \\ L(\mathtt{n}) = L(0) + \frac{h}{\Gamma(\kappa_2)} \sum_{\mathtt{j}=1}^{\mathtt{n}} \frac{\Gamma(\mathtt{n}-\mathtt{j}+\kappa_2)}{\Gamma(\mathtt{n}-\mathtt{j}+1)} & [\beta S(\mathtt{j}-1)(L(\mathtt{j}-1) + B(\mathtt{j}-1)) \\ & -\gamma_1 L(\mathtt{j}-1) - \alpha L(\mathtt{j}-1) - \sigma L(\mathtt{j}-1)], \\ B(\mathtt{n}) = B(0) + \frac{h}{\Gamma(\kappa_3)} \sum_{\mathtt{j}=1}^{\mathtt{n}} \frac{\Gamma(\mathtt{n}-\mathtt{j}+\kappa_3)}{\Gamma(\mathtt{n}-\mathtt{j}+1)} & [\alpha L(\mathtt{j}-1) - \gamma_2 B(\mathtt{j}-1) - \sigma B(\mathtt{j}-1)], \end{cases} \tag{12}$$

where the initial conditions are $S(0), L(0)$, and $B(0)$.

Numerical simulations can be used to analyze the dynamics of system (11) and comprehend its behavior. Bifurcation diagrams, phase portraits, and the maximum Lyapunov exponent (MLE) (computed using the Jacobian matrix algorithm Wu & Baleanu (2015)) are three essential tools for this analysis. For the incommensurate system (11), the fractional order κ_3 plays a crucial role in shaping the nonlinear dynamics of the fractional computer virus model. To investigate its effect, we fix the orders at $\kappa_1 = 0.8$, $\kappa_2 = 1$, and vary κ_3 in the range $[0.65, 1]$ with initial values $(0.4, 0.4, 0.2)$ and take $\sigma = 0.1$, $\beta = 2.1$, $\gamma_1 = 0.1$, $\gamma_2 = 0.3$, and $\alpha = 1.9$. The results are illustrated in Figure 1. In Figure 1(a), the phase portrait shows a strange attractor with a dense and irregular structure, confirming the existence of persistent chaotic oscillations rather than convergence to equilibrium or periodic cycles. This reflects the strong nonlinear interaction among susceptible, latent, and breaking nodes under incommensurate memory effects. The incommensurate fractional orders are chosen as $\kappa_1 = 0.8$, $\kappa_2 = 1$, and $\kappa_3 = 0.67$. These values are selected to illustrate the sensitivity of the system to variations in fractional orders. Numerical bifurcation analysis and the computation of the maximum Lyapunov exponent (MLE) indicate that these orders produce pronounced chaotic windows, enabling an effective investigation of both chaotic dynamics and synchronization phenomena. This choice also demonstrates the richer dynamical behavior achievable in the incommensurate fractional-order system compared to commensurate or integer-order models. The bifurcation diagram in Figure 1(b) reveals that as κ_3 increases, the system undergoes a transition from relatively narrow chaotic bands to wider, more dispersed regions, interspersed with periodic windows. This widening indicates a higher level of unpredictability and irregular fluctuations in the susceptible population as the order approaches unity. The MLE curve in Figure 1(c) remains positive throughout the considered interval, with values rising to approximately 0.42 near $\kappa_3 = 1$. This confirms the presence of robust chaos and demonstrates that the instability of trajectories strengthens with increasing κ_3. The positive MLE provides a quantitative validation of the chaotic attractors observed in 1(a) and the bifurcation structures in 1(b). These results demonstrate that the incommensurate-order formulation of the fractional discrete computer virus model exhibits rich chaotic behavior for most values of κ_3. This highlights the sensitive dependence of the system on memory asymmetry: even when one fractional order is fixed at unity, varying the other orders can significantly alter the complexity of virus propagation dynamics.

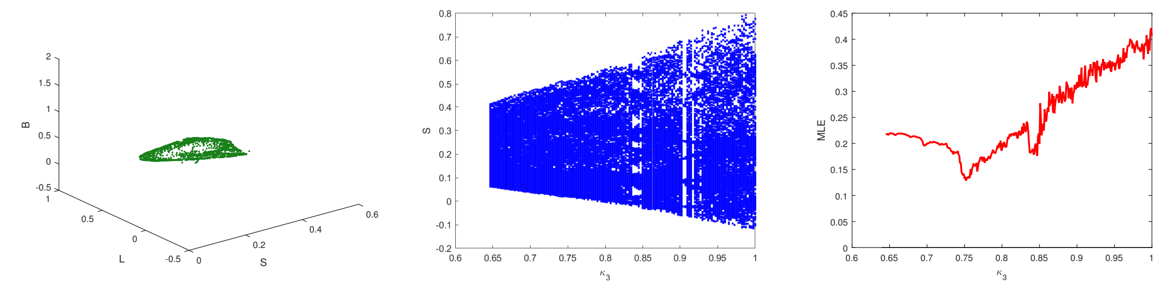

(a) **(b)** **(c)**

Figure 1: Incommensurate fractional discrete computer virus dynamics. (a) Chaotic attractor in (S, L, B) for $(\kappa_1, \kappa_2, \kappa_3) = (0.8, 1, 0.67)$. (b) Bifurcation diagram of S versus the third fractional order κ_3. (c) Largest Lyapunov exponent (MLE) versus κ_3.

In the present study, the model parameters are chosen for illustrative purposes to elucidate the system's chaotic dynamics and synchronization behavior. In practical applications, however, these parameters, such as infection, recovery, and coupling rates, can be estimated from real-world data. For instance, epidemiological models adapted to malware spread have been fitted to real malware datasets to infer infection and recovery rates (Yom-Tov et al., 2019). Similarly, studies using Monte Carlo or Physics-Informed Neural Network (PINN) approaches have demonstrated effective estimation of critical parameters (e.g., infection rate, removal rate) in malware propagation models within IoT networks (Severt, Casado-Vara & Martín del Rey, 2023). We emphasize that integrating real data-driven calibration into our fractional-order framework is a promising direction for future work.

3 Synchronization Result

This section focuses on the synchronization of fractional-order chaotic computer virus models. We design an adaptive control scheme to force the synchronization error between two systems to converge to zero.

The master system is described as

$$\begin{cases} {}^{\mathtt{c}}\Delta_b^{\kappa_1} S(\mathtt{t}) &= \sigma - \beta S(\mathtt{t}+\kappa_1-1)(L(\mathtt{t}+\kappa_1-1)+B(\mathtt{t}+\kappa_1-1)) + \gamma_1 L(\mathtt{t}+\kappa_1-1) \\ &\quad +\gamma_2 B(\mathtt{t}+\kappa_1-1) - \sigma S(\mathtt{t}+\kappa_1-1), \\ {}^{\mathtt{c}}\Delta_b^{\kappa_2} L(\mathtt{t}) &= \beta S(\mathtt{t}+\kappa_2-1)(L(\mathtt{t}+\kappa_2-1)+B(\mathtt{t}+\kappa_2-1)) - \gamma_1 L(\mathtt{t}+\kappa_2-1) \\ &\quad -\alpha L(\mathtt{t}+\kappa_2-1) - \sigma L(\mathtt{t}+\kappa_2-1), \\ {}^{\mathtt{c}}\Delta_b^{\kappa_3} B(\mathtt{t}) &= \alpha L(\mathtt{t}+\kappa_3-1) - \gamma_2 B(\mathtt{t}+\kappa_3-1) - \sigma B(\mathtt{t}+\kappa_3-1). \end{cases} \tag{13}$$

and the controlled incommensurate system is given by

$$\begin{cases} {}^{\mathtt{c}}\Delta_b^{\kappa_1} S_s(\mathtt{t}) &= \sigma - \beta S_s(\mathtt{t}+\kappa_1-1)(L_s(\mathtt{t}+\kappa_1-1)+B_s(\mathtt{t}+\kappa_1-1)) + \gamma_1 L_s(\mathtt{t}+\kappa_1-1) \\ &\quad +\gamma_2 B_s(\mathtt{t}+\kappa_1-1) - \sigma S_s(\mathtt{t}+\kappa_1-1) + T_1(\mathtt{t}+\kappa_1-1), \\ {}^{\mathtt{c}}\Delta_b^{\kappa_2} L_s(\mathtt{t}) &= \beta S_s(\mathtt{t}+\kappa_2-1)(L_s(\mathtt{t}+\kappa_2-1)+B_s(\mathtt{t}+\kappa_2-1)) - \gamma_1 L_s(\mathtt{t}+\kappa_2-1) \\ &\quad -\alpha L_s(\mathtt{t}+\kappa_2-1) - \sigma L_s(\mathtt{t}+\kappa_2-1) + T_2(\mathtt{t}+\kappa_2-1), \\ {}^{\mathtt{c}}\Delta_b^{\kappa_3} B_s(\mathtt{t}) &= \alpha L_s(\mathtt{t}+\kappa_3-1) - \gamma_2 B_s(\mathtt{t}+\kappa_3-1) - \sigma B_s(\mathtt{t}+\kappa_3-1) + T_3(\mathtt{t}+\kappa_3-1). \end{cases} \tag{14}$$

where the control inputs $T_1(t)$, $T_2(t)$, and $T_3(t)$ are designed to synchronize the two systems. Now, define the error states as $e_1 = S_s - S$, $e_2 = L_s - L$ and $e_3 = B_s - B$. The resulting error dynamics system can be obtained by

$$\begin{cases} {}^{\mathtt{c}}\Delta_b^{\kappa_1} e_1(\mathtt{t}) &= -\beta S_s(\mathtt{t}+\kappa_1-1)(L_s(\mathtt{t}+\kappa_1-1)+B_s(\mathtt{t}+\kappa_1-1)) + \gamma_1 L_s(\mathtt{t}+\kappa_1-1) \\ &\quad +\gamma_2 B_s(\mathtt{t}+\kappa-1) - \sigma S_s(\mathtt{t}+\kappa_1-1) + T_1(\mathtt{t}+\kappa_1-1) \\ &\quad +\beta S(\mathtt{t}+\kappa_1-1)(L(\mathtt{t}+\kappa_1-1)+B(\mathtt{t}+\kappa_1-1)) - \gamma_1 L(\mathtt{t}+\kappa_1-1) \\ &\quad -\gamma_2 B(\mathtt{t}+\kappa_1-1) + \sigma S(\mathtt{t}+\kappa_1-1), \\ {}^{\mathtt{c}}\Delta_b^{\kappa_2} e_2(\mathtt{t}) &= \beta S_s(\mathtt{t}+\kappa_2-1)(L_s(\mathtt{t}+\kappa_2-1)+B_s(\mathtt{t}+\kappa_2-1)) - \gamma_1 L_s(\mathtt{t}+\kappa_2-1) \\ &\quad -\alpha L_s(\mathtt{t}+\kappa_2-1) - \sigma L_s(\mathtt{t}+\kappa_2-1) + T_2(\mathtt{t}+\kappa_2-1) \\ &\quad -\beta S(\mathtt{t}+\kappa_2-1)(L(\mathtt{t}+\kappa_2-1)+B(\mathtt{t}+\kappa_2-1)) + \gamma_1 L(\mathtt{t}+\kappa_2-1) \\ &\quad +\alpha L(\mathtt{t}+\kappa_2-1) + \sigma L(\mathtt{t}+\kappa_2-1), \\ {}^{\mathtt{c}}\Delta_b^{\kappa_3} e_3(\mathtt{t}) &= \alpha L_s(\mathtt{t}+\kappa_3-1) - \gamma_2 B_s(\mathtt{t}+\kappa_3-1) - \sigma B_s(\mathtt{t}+\kappa_3-1) + T_3(\mathtt{t}+\kappa_3-1) \\ &\quad -\alpha L(\mathtt{t}+\kappa_3-1) + \gamma_2 B(\mathtt{t}+\kappa_3-1) + \sigma B(\mathtt{t}+\kappa_3-1). \end{cases} \tag{15}$$

The following theorem establishes adaptive rules for the controllers T_1, T_2, and T_3, ensuring that the synchronization error asymptotically converges to zero.

Theorem 3. *Subject to*

$$\begin{cases} T_1(\mathtt{t}) & = f_1 e_1(\mathtt{t}) + \beta(-S(\mathtt{t})(L(\mathtt{t}) + B(\mathtt{t})) + S_s(\mathtt{t})(L_s(\mathtt{t}) + B_s(\mathtt{t}))) + \gamma_1(L(\mathtt{t}) - L_s(\mathtt{t})) \\ & \quad +\gamma_2(B(\mathtt{t}) - B_s(\mathtt{t})) - \sigma(S_s(\mathtt{t}) - S(\mathtt{t})), \\ T_2(\mathtt{t}) & = f_2 e_2(\mathtt{t}) + \beta(S(\mathtt{t})(L(\mathtt{t}) + B(\mathtt{t})) - S_s(\mathtt{t})(L_s(\mathtt{t}) + B_s(\mathtt{t}))) \\ & \quad -(\gamma_1 - \alpha - \sigma)(L(\mathtt{t}) - L_s(\mathtt{t}))), \\ T_3(\mathtt{t}) & = f_3 e_3(\mathtt{t}) + \alpha(L(\mathtt{t}) - L_s(\mathtt{t})) - (\gamma_2 + \sigma)(B(\mathtt{t}) - B_s(\mathtt{t})), \end{cases} \tag{16}$$

The master system (13) *and slave systems* (14) *achieve synchronization at* $f_1 = -0.34, f_2 = -0.52$ *and* $f_3 = -0.76$

Proof. Substituting T_1, T_2, and T_3 into (15), the following error dynamical system is obtained:

$$\begin{cases} {}^{\mathtt{c}}\Delta_b^{\kappa_1} e_1(\mathtt{t}) = f_1 e_1(\mathtt{t}), \\ {}^{\mathtt{c}}\Delta_b^{\kappa_2} e_2(\mathtt{t}) = f_2 e_2(\mathtt{t}), \\ {}^{\mathtt{c}}\Delta_b^{\kappa_3} e_3(\mathtt{t}) = f_3 e_3(\mathtt{t}). \end{cases} \tag{17}$$

Applying Theorem 2, the corresponding stability condition is given by:

$$\det\left(\mathrm{diag}(\lambda^{M\kappa_1}, \lambda^{M\kappa_2}, \lambda^{M\kappa_3}) - (1 - \lambda^M)\mathcal{A}\right) = 0, \tag{18}$$

where $M = 100$ for $(\kappa_1, \kappa_2, \kappa_3) = (0.8, 1, 0.67)$.

Explicitly, we obtain:

$$\det\left(\begin{pmatrix} \lambda^{80} & 0 & 0 \\ 0 & \lambda^{100} & 0 \\ 0 & 0 & \lambda^{67} \end{pmatrix} - (1 - \lambda^{100})\begin{pmatrix} f_1 & 0 & 0 \\ 0 & f_2 & 0 \\ 0 & 0 & f_3 \end{pmatrix}\right) = 0, \tag{19}$$

which reduces to:

$$\left(\lambda^{80} - f_1(1 - \lambda^{100})\right)\left(\lambda^{100} - f_2(1 - \lambda^{100})\right)\left(\lambda^{67} - f_3(1 - \lambda^{100})\right) = 0, \tag{20}$$

The control inputs $f_1 = -0.34, f_2 = -0.52$, and $f_3 = -0.76$ are designed to stabilize the error system, driving the error states in (17) to zero. The 300 solutions λ_j $(j = 1, \ldots, 300)$ of Equation (20) all lie in $\mathbb{C} \setminus K^{\frac{1}{100}}$, ensuring that the stability criterion of Theorem 2 is satisfied. Consequently, the error dynamics (17) are asymptotically stable. The rapid convergence of the errors in (17) to zero establishes synchronization between the master system (13) and the slave system (14). This theoretical result is supported by Figure 2, where the error states converge to zero under the designed control inputs and the incommensurate orders $\kappa_1 = 0.8, \kappa_2 = 1$, and $\kappa_3 = 0.67$. □

4 Conclusion and Future Works

In this work, we investigated the chaotic dynamics and synchronization of an incommensurate fractional discrete computer virus model, which incorporates memory effects and non-local behavior inherent in real-world networks. The system's complex behavior was characterized using bifurcation diagrams, phase portraits, and the maximum Lyapunov exponent (MLE), confirming chaotic regimes where $MLE > 0$. A master–slave coupling strategy was implemented to achieve synchronization in the chaotic regime, and the convergence of the synchronization error was quantified. Numerical simulations showed that the master and slave systems synchronize effectively for specific control parameters. The results highlight how incommensurate fractional orders shape chaotic windows and demonstrate that appropriately tuned feedback can enforce

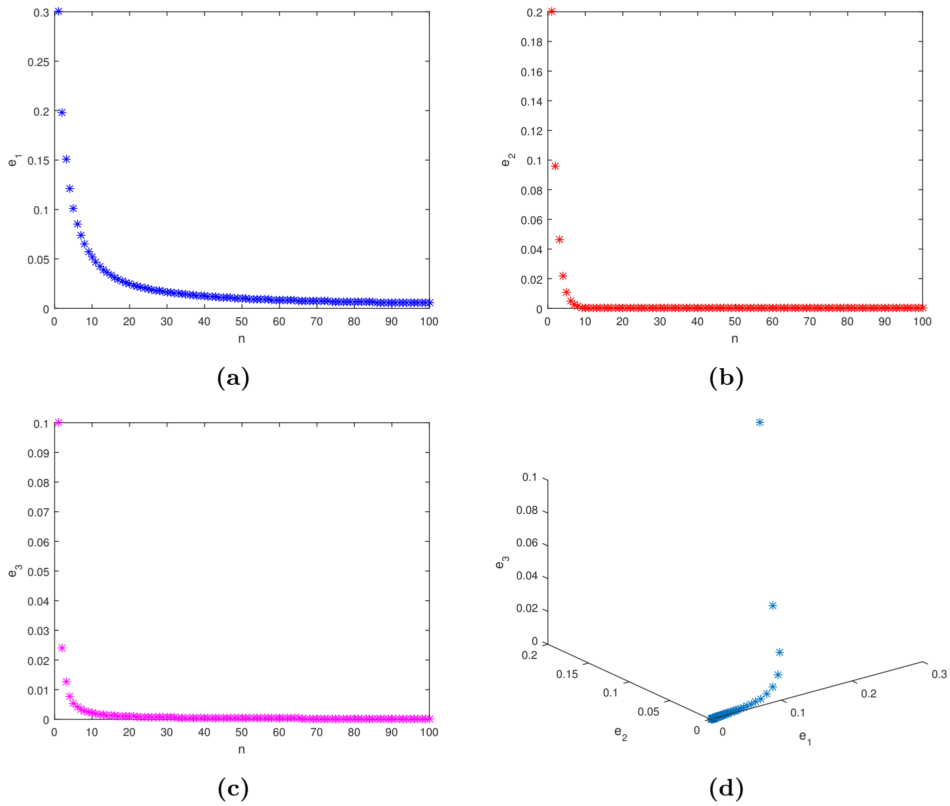

Figure 2: Evolution of the incommensurate error system (17) for $(\kappa_1, \kappa_2, \kappa_3) = (0.8, 1, 0.67)$ and $(e_1(0), e_2(0), e_3(0)) = (0.3, 0.2, 0.1)$.

coherent behavior, offering insights for the design of mitigation strategies against computer-virus propagation in complex networks. In addition to contributing to the growing body of research on fractional-order systems, this work provides practical information for developing countermeasures against digital epidemics. Future research could extend the model to incorporate network topologies, time delays, adaptive control, and real-world data calibration. We appreciate the reviewer's suggestion that calibrating the model with real-world malware propagation data would further enhance practical relevance; due to limited dataset availability, this is proposed as a promising direction for future work.

Acknowledgment

The authors would like to express their sincere gratitude to Ajman University for its generous support in covering the publication fee and facilitating the completion of this research.

References

Abdeljawad, T. (2011). On Riemann and Caputo fractional differences. *Comput. Math. Appl.*, *62*, 1602–1611.

Anakira, N. R., Almalki, A., Katatbeh, D., Hani, G. B., Jameel, A. F., Al Kalbani, K. S., & Abu-Dawas, M. (2023). An algorithm for solving linear and non-linear Volterra integro-differential equations. *Int. J. Adv. Soft Comput. Appl.*, *15*(3), 70–83.

Atici, F. M., & Eloe, P. (2009). Discrete fractional calculus with the nabla operator. *Electron. J. Qual. Theory Differ. Equ.*, *2009*, Paper 3.

Bendoukha, S., Ouannas, A., Wang, X., Khennaoui, A.-A., Pham, V.-T., Grassi, G., & Huynh, V. V. (2018). The co-existence of different synchronization types in fractional-order discrete-time chaotic systems with non-identical dimensions and orders. *Entropy*, *20*(9), 710.

Berir, M. (2024). Analysis of the effect of white noise on the Halvorsen system of variable-order fractional derivatives using a novel numerical method. *Int. J. Adv. Soft Comput. Appl.*, *16*(3), 294–306.

Batiha, I., Anakira, N., Bendib, I., Ouannas, A., Hioual, A., Irianto, I., & Amourah, A. (2025a). Finite-time analysis of epidemic reaction-diffusion models: Stability, synchronization, and numerical insights. *PLoS One*, *20*(5), e0321132.

Batiha, I. M., Bendib, I., Ouannas, A., Agarwal, P., Anakira, N., Jebril, I. H., & Momani, S. (2025b). Finite-time synchronization in a novel discrete fractional SIR model for COVID-19. *Boletim da Sociedade Paranaense de Matemática*, *43*(1), 1–15.

Cuomo, K. M., & Oppenheim, A. V. (1993). Circuit implementation of synchronized chaos with applications to communications. *Phys. Rev. Lett.*, *71*(1), 65–68.

Dharmalingam, K. M., Jeeva, N., Ali, N., Al-Hamido, R. K., Fadugba, S. E., Malesela, K., Tolasa, F. T., El-Bahkiry, H. S., & Qousini, M. (2024). Mathematical analysis of Zika virus transmission: Exploring semi-analytical solutions and effective controls. *Commun. Math. Biol. Neurosci.*, *2024*, Article 112.

Farraj, G., Maayah, B., Khalil, R., & Beghami, W. (2023). An algorithm for solving fractional differential equations using conformable optimized decomposition method. *Int. J. Adv. Soft Comput. Appl.*, *15*(1), 187–196.

Khennaoui, A. A., Ouannas, A., Bendoukha, S., Grassi, G., Lozi, R. P., & Pham, V.-T. (2019). On fractional–order discrete–time systems: Chaos, stabilization and synchronization. *Chaos Solitons Fractals*, *119*, 150–162.

Khennaoui, A. A., Ouannas, A., Bendoukha, S., Grassi, G., Wang, X., Pham, V.-T., & Alsaadi, F. E. (2018). Generalized and inverse generalized synchronization of fractional-order discrete-time chaotic systems with non-identical dimensions. *Adv. Differ. Equ.*, *2018*, 303.

Khennaoui, A. A., Ouannas, A., Bendoukha, S., Grassi, G., Wang, X., Pham, V.-T., & Alsaadi, F. E. (2019). Chaos, control, and synchronization in some fractional-order difference equations. *Adv. Differ. Equ.*, *2019*, 412.

Liu, Y. (2016). Chaotic synchronization between linearly coupled discrete fractional Hénon maps. *Indian J. Phys.*, *90*(3), 313–317.

Momani, S., Batiha, I. M., Bendib, I., Ouannas, A., Hioual, A., & Mohamed, D. (2025). Examining finite-time behaviors in the fractional Gray–Scott model: Stability, synchronization, and simulation analysis. *International Journal of Cognitive Computing in Engineering*, *6*, 380–390.

Ouannas, A., Batiha, I. M., & Pham, V.-T. (2023). *Fractional Discrete Chaos: Theories, Methods and Applications.* World Scientific.

Ouannas, A., Khennaoui, A. A., Batiha, I. M., & Pham, V.-T. (2022). Synchronization between fractional chaotic maps with different dimensions. In A. G. Radwan, F. A. Khanday, & L. A. Said (Eds.), *Fractional-Order Design: Emerging Methodologies and Applications in Modelling* (Vol. 3, pp. 89–121). Academic Press.

Ouannas, A., Bendoukha, S., Khennaoui, A. A., Grassi, G., Wang, X., & Pham, V.-T. (2019a). Chaos synchronization of fractional–order discrete–time systems with different dimensions using two scaling matrices. *Open Phys.*, *17*(1), 942–949.

Ouannas, A., Grassi, G., Azar, A. T., Khennaoui, A. A., & Pham, V.-T. (2020). Synchronization of fractional-order discrete-time chaotic systems. In A. E. Hassanien, K. Shaalan, & M. F. Tolba (Eds.), *Adv. Intell. Syst. Comput.*, *1058*, 218–228. Springer, Cham.

Ouannas, A., Bendoukha, S., Karouma, A., & Abdelmalek, S. (2019b). A general method to study the co-existence of different hybrid synchronizations in fractional-order chaotic systems. *Int. J. Nonlinear Sci. Numer. Simul.*, *20*(3–4), 351–359.

Ouannas, A., Pham, V.-T. (2019). New trends in synchronization of fractional-order chaotic systems. In I. Petráš (Ed.), *Handbook of Fractional Calculus with Applications, Vol. 6: Applications in Control* (pp. 397–422). De Gruyter.

Ouannas, A., Debbouche, N., Wang, X., Pham, V.-T., & Zehrour, O. (2018). Secure multiple-input multiple-output communications based on F–M synchronization of fractional-order chaotic systems with non-identical dimensions and orders. *Appl. Sci.*, *8*(10), 1746.

Ouannas, A., Odibat, Z. (2015a). Generalized synchronization of different dimensional chaotic dynamical systems in discrete time. *Nonlinear Dyn.*, *81*(1), 765–771.

Ouannas, A., Azar, A. T., & Vaidyanathan, S. (2017). A robust method for new fractional hybrid chaos synchronization. *Math. Methods Appl. Sci.*, *40*(5), 1804–1812.

Ouannas, A., Odibat, Z. (2015b). Generalized synchronization of different dimensional chaotic dynamical systems in discrete time. *Nonlinear Dyn.*, *81*(1), 765–771.

Ouannas, A., & Al-Sawalha, M. M. (2016). Synchronization between different dimensional chaotic systems using two scaling matrices. *Optik*, *127*(2), 959–963.

Ouannas, A., Khennaoui, A. A., Odibat, Z., Pham, V.-T., & Grassi, G. (2019c). On the dynamics, control, and synchronization of the fractional-order Ikeda map. *Chaos Solitons Fractals*, *123*, 108–115.

Ouannas, A., Khennaoui, A. A., Zehrour, O., Bendoukha, S., Grassi, G., & Pham, V.-T. (2019d). Synchronisation of integer-order and fractional-order discrete-time chaotic systems. *Pramana*, *92*(4), 52.

Ren, J., Yang, X., Zhu, Q., Yang, L.-X., & Zhang, C. (2012). A novel computer virus model and its dynamics. *Nonlinear Anal.: Real World Appl.*, *13*(1), 376–384.

Shatnawi, M. T., Djenina, N., Ouannas, A., Batiha, I. M., & Grassi, G. (2022). Novel convenient conditions for the stability of nonlinear incommensurate fractional-order difference systems. *Alex. Eng. J.*, *61*, 1655–1663.

Severt, M., Casado-Vara, R., & Martín del Rey, Á. (2023). A comparison of Monte Carlo-based and PINN parameter estimation methods for malware identification in IoT networks. *Technologies*, *11*(5), 133.

Talbi, I., Ouannas, A., Khennaoui, A. A., Berkane, A., Batiha, I. M., Grassi, G., & Pham, V.-T. (2020a). Different dimensional fractional-order discrete chaotic systems based on the Caputo h-difference discrete operator: dynamics, control, and synchronization. *Adv. Differ. Equ.*, *2020*, 624.

Talbi, I., Ouannas, A., Grassi, G., Khennaoui, A. A., Pham, V.-T., & Baleanu, D. (2020b). Fractional Grassi–Miller map based on the Caputo h-difference operator: Linear methods for chaos control and synchronization. *Discrete Dyn. Nat. Soc.*, *2020*, Article ID 8825694.

Terry, J. R., VanWiggeren, G. D. (2001). Chaotic communication using generalized synchronization. *Chaos Solitons Fractals*, *12*(1), 145–152.

Wu, G.-C., Baleanu, D. (2014). Chaos synchronization of the discrete fractional logistic map. *Signal Process.*, *102*, 96–99.

Wu, G.-C., Baleanu, D., Xie, H.-P., & Chen, F.-L. (2016). Chaos synchronization of fractional chaotic maps based on the stability condition. *Physica A: Statistical Mechanics and its Applications*, *460*, 374–383.

Wu, G.-C., Baleanu, D. (2014). Discrete fractional logistic map and its chaos. *Nonlinear Dyn.*, *75*, 283–287.

Wu, G.-C., & Baleanu, D. (2015). Jacobian matrix algorithm for Lyapunov exponents of the discrete fractional maps. *Commun. Nonlinear Sci. Numer. Simul.*, *22*, 95–100.

Yom-Tov, E., Levy, N., & Rubin, A. (2019). Modeling infection methods of computer malware in the presence of vaccinations using epidemiological models: An analysis of real-world data. *arXiv*, arXiv:1908.09902.

Yang, L.-X., Yang, X. (2012). The spread of computer viruses under the influence of removable storage devices. *Appl. Math. Comput.*, *219*(8), 3914–3922.

Yang, L.-X., Yang, X., Zhu, Q., & Wen, L. (2013). A computer virus model with graded cure rates. *Nonlinear Anal.: Real World Appl.*, *14*(1), 414–422.

Zhang, G., Liu, Z., & Ma, Z. (2007). Generalized synchronization of different dimensional chaotic dynamical systems. *Chaos Solitons Fractals*, *32*(2), 773–779.